Published OnlineFirst March 9, 2010; DOI: 10.1158/0008-5472.CAN-09-2840

Tumor and Stem Cell Biology

Cancer Research

Constitutively Active Stat3 Enhances Neu-Mediated Migration and Metastasis in Mammary Tumors via Upregulation of Cten

Isaia Barbieri[1,2], Sara Pensa[1,2], Tania Pannellini[4], Elena Quaglino[1,3], Diego Maritano[1,2], Marco Demaria[1,2], Alessandra Voster[1,2], James Turkson[6], Federica Cavallo[1,3], Christine J. Watson[5], Paolo Provero[1,2], Piero Musiani[4], and Valeria Poli[1,2]

Abstract

The transcription factor signal transducer and activator of transcription 3 (STAT3) is constitutively activated in tumors of different origin, but the molecular bases for STAT3 requirement are only partly understood. To evaluate the contribution of enhanced Stat3 activation in a controlled model system, we generated knock-in mice wherein a mutant constitutively active *Stat3C* allele replaces the endogenous wild-type allele. Stat3C could enhance the tumorigenic power of the rat *Neu* oncogene in mouse mammary tumor virus (MMTV)–Neu transgenic mice, triggering the production of earlier onset, more invasive mammary tumors. Tumor-derived cell lines displayed higher migration, invasion, and metastatic ability and showed disrupted distribution of cell-cell junction markers mediated by Stat3-dependent overexpression of the COOH terminal tensin-like (Cten) focal adhesion protein, which was also significantly upregulated in Stat3C mammary tumors. Importantly, the proinflammatory cytokine interleukin-6 could mediate Cten induction in MCF10 cells in an exquisitely Stat3-dependent way, showing that Cten upregulation is a feature of inflammation-activated Stat3. In light of the emerging pivotal role of Stat3 in connecting inflammation and cancer, our identification of Cten as a Stat3-dependent mediator of migration provides important new insights into the oncogenic role of Stat3, particularly in the breast. *Cancer Res; 70(6); 2558–67. ©2010 AACR.*

Introduction

The latent signal transducer and activator of transcription 3 (STAT3) transcription factor can be activated by a wide variety of cytokines and by a number of growth factors and oncogenes, including c-Src, epidermal growth factor receptor (EGFR), and ErbB-2, defined as HER2 in humans and Neu in the rat (1, 2). Accordingly, STAT3 is found to be constitutively active in a high percentage of human and mouse tumors and tumor-derived cell lines of both hematologic and solid origin, which often become addicted to its activity for continuous survival and growth (3, 4). Known STAT3 activities that can contribute to tumorigenesis include enhancing tumor cell proliferation and survival, downmodulating antitumor immune responses, promoting angiogenesis, and inducing cell movement and epithelial-to-mesenchymal transition (EMT; refs. 5, 6). Moreover, an important role for this factor in linking inflammation and cancer downstream of autocrine or paracrine production of interleukin-6 (IL-6) has recently emerged (7).

The prooncogenic role of STAT3 was shown by the finding that overexpression of the constitutively active mutant form Stat3C can transform cultured cells (8–10). Recently, *in vivo* Stat3C overexpression was shown to enhance malignant progression of skin tumors (11) or to trigger the onset of lung adenocarcinomas (12). Despite the efforts of many laboratories, the mechanisms underlying *in vivo* STAT3 prooncogenic activities are however still incompletely understood. Indeed, many of its known proproliferative or antiapoptotic target genes have been identified upon acute stimulation and are not consistently induced in tumors displaying lower but continuous Stat3 phosphorylation, suggesting that distinct repertoires of target genes may be induced under these two conditions. Thus, overexpression and/or acute stimulation does not seem to be the best

Authors' Affiliations: [1]Molecular Biotechnology Center, [2]Department of Genetics, Biology and Biochemistry, and [3]Department of Clinical and Biological Sciences, University of Turin, Turin, Italy; [4]Aging Research Center, "G. d'Annunzio" University Foundation, Chieti, Italy; [5]Department of Pathology, University of Cambridge, Cambridge, United Kingdom; and [6]Department of Molecular Biology and Microbiology, University of Central Florida, Orlando, Florida

Note: Supplementary data for this article are available at Cancer Research Online (http://cancerres.aacrjournals.org/).

I. Barbieri and S. Pensa contributed equally to this work.

Present address for D. Maritano: Azienda Ospedaliera Santa Croce e Carle, Via Coppino 26, 12100 Cuneo, Italy.

Present address for A. Voster: Merck Serono S.A.-Istituto di Ricerche Biomediche "A. Marxer," RBM SpA, Via Ribes 1, 10010 Colleretto Giacosa, Turin, Italy.

Corresponding Author: Valeria Poli, University of Turin, Via Nizza 52, 10126 Turin, Italy. Phone: 39-011-6706428; Fax: 39-011-6706432; E-mail: valeria.poli@unito.it.

doi: 10.1158/0008-5472.CAN-09-2840

Published OnlineFirst March 9, 2010; DOI: 10.1158/0008-5472.CAN-09-2840

experimental system to assess the Stat3 prooncogenic functions *in vivo*.

Mammary tumors often display STAT3 constitutive activity, which is required for continuous proliferation and resistance to apoptosis of tumor-derived cells (13–15) and correlates with high expression of the EGFR family members EGFR and/or HER2 (13, 16, 17). The *HER2* oncogene is often amplified in human mammary tumors, particularly those displaying loss of estrogen sensitivity and poor prognosis (18). Accordingly, overexpression of the rat oncogenic form Neu in the mammary gland of mouse mammary tumor virus (MMTV)–*Neu* transgenic mice (NeuT) triggers the onset of invasive multifocal breast carcinomas (19) and is widely used as a model for human breast cancer (20). Recently, both we and others have shown that Stat3 is not required for Neu-mediated tumorigenesis but is essential for metastasis formation, both *in vivo* and *in vitro* (21, 22). Defective metastatic ability could be ascribed both to altered expression of proangiogenic and inflammatory genes, leading to impaired angiogenic and inflammatory responses (22), and to cell autonomous defects in anchorage-independent growth (21).

Here, we address some of the outstanding questions about which role constitutively active Stat3 plays *in vivo* by generating knock-in mice wherein a mutant *Stat3C* allele replaces the wild-type endogenous gene and assessing its prooncogenic activity in the context of Neu-mediated mammary tumorigenesis, providing important insights into the molecular mechanisms involving Stat3 in breast cancer.

Materials and Methods

Animals, treatments, and analysis. Mice were maintained in the transgenic unit of the Molecular Biotechnology Center (University of Turin) under a 12-h light-dark cycle and provided food and water *ad libitum*. Procedures were conducted in conformity with national and international laws and policies as approved by the Faculty Ethical Committee. *Stat3*$^{C/WT}$ female mice were bred to NeuT males to generate the NeuT;*Stat3*$^{C/WT}$ or NeuT;*Stat3*$^{WT/WT}$ littermates used, thereby called N-C or N-WT. Palpable tumor onset was assessed in blind by weekly palpation. Mice were sacrificed by cervical dislocation.

Cell lines derivation and culture. Tumor cell lines were isolated from three different N-C and N-WT mice as described (23), subjected to differential trypsinization to eliminate fibroblasts, cultured in complete medium (RPMI 1360, 20% FCS, 2 mmol/L Glutamax, 100 units/mL penicillin, and 100 μg/mL streptomycin) and passaged with 0.05% trypsin-EDTA. MCF10A cells, cultured as previously described (24), were obtained from American Type Culture Collection and routinarily tested for *Mycoplasma* infection, morphology under both subconfluent and confluent conditions by phase contrast microscopy, and the ability to undergo EMT. For IL-6 or EGF treatments, cells were starved from serum and EGF overnight and then treated with recombinant IL-6 (500 ng/mL) plus soluble IL-6 receptor (250 ng/mL) as previously described (25) or with 10 ng/mL human recombinant EGF (Sigma-Aldrich) with or without pretreatment overnight with 100 μmol/L Stat3 inhibitor S3I-201 (26). C1 cells received 200 μmol/L S3I-201.

Transwell invasion and migration assays. Cells (1×10^5) were placed in serum-free medium on Transwell inserts coated or not with 2 μg of Matrigel (BD Biosciences). After incubation in wells containing RPMI ± 20% FCS, inserts were stained with Diff Quick Staining Set (Medion Diagnostic) and cells on the lower surface counted in blind.

S.c. tumors and lung metastasis. Cells (1×10^5) were injected into the right fat pad or into the tail vein of nude CD1 female mice. S.c. tumors were measured with a caliper weekly, and mice were sacrificed whenever the tumor exceeded 10 mm of diameter. I.v. injected mice were sacrificed after 3 or 5 wk; lungs were fixed with 2% paraformaldehyde, 0.1 mol/L L-lysine, and 10 mmol/L sodium metaperiodate. Semiserial sections at 100-μm intervals were stained with H&E, and neoplastic lesions were counted in blind.

Western blots. Total and nuclear protein extracts were obtained as previously described (25, 27). Samples were fractionated on SDS-PAGE and transferred to a polyvinylidene difluoride membrane (Millipore).

Whole-mount image analyses. Images of whole-mount (WM) preparations were taken with a Nikon Coolpix 950 digital camera (Nital Spa) mounted on a stereoscopic Leica MZ 6 microscope (Leica Microsystems). Specific instrument settings and quantification protocol are reported in Supplementary Data.

RNA extraction and analysis. Total RNA was extracted with Trizol reagent (Invitrogen) and purified using Invitrogen Micro-to-Midi Total RNA Purification System (Invitrogen). Reverse transcription and real-time PCR were performed as described (24, 28) using the ABI Prism 7300 Real-Time PCR System (Applied Biosystems) and the Universal Probe Library (Roche Italia) probes.

COOH terminal tensin-like silencing. Cells were plated at a density of 60% in 24-well plates or on coverslips for immunofluorescence analysis and incubated for 72 h with 1 μmol/L Accell SMARTpool siRNA (E-054907-00) or with the Accell nontargeting siRNA (D-001910-01-05, Dharmacon, Thermo Fisher Scientific) in SMARTpool delivery medium according to manufacturer's protocol. As a control for siRNA entry, cells were incubated in parallel with an Accell Green nontargeting siRNA (D-001950-01), and a glyceraldehyde-3-phosphate dehydrogenase–targeting siRNA was used as positive control. Fluorescence-positive cells were ~90% for all experiments.

Antibodies. Rabbit polyclonal against p-Stat3 or p-Stat5 (Cell Signaling Technology), Stat3 or Stat5 (Santa Cruz Biotechnology), and zonula occludens-1 (Zo-1; Zymed). Mouse monoclonal against β-catenin (BD Biosciences), vinculin (Sigma-Aldrich), E-cadherin 5H9 (Millipore), and proliferating cell nuclear antigen (PCNA; Ylem). Antihuman COOH terminal tensin-like (CTEN; ref. 29) was a kind gift from Prof. S.H. Lo (University of California-Davis); antimouse Cten was generated in house by immunization with a MBP-Cten fusion protein and purified against the recombinant protein.

Published OnlineFirst March 9, 2010; DOI: 10.1158/0008-5472.CAN-09-2840

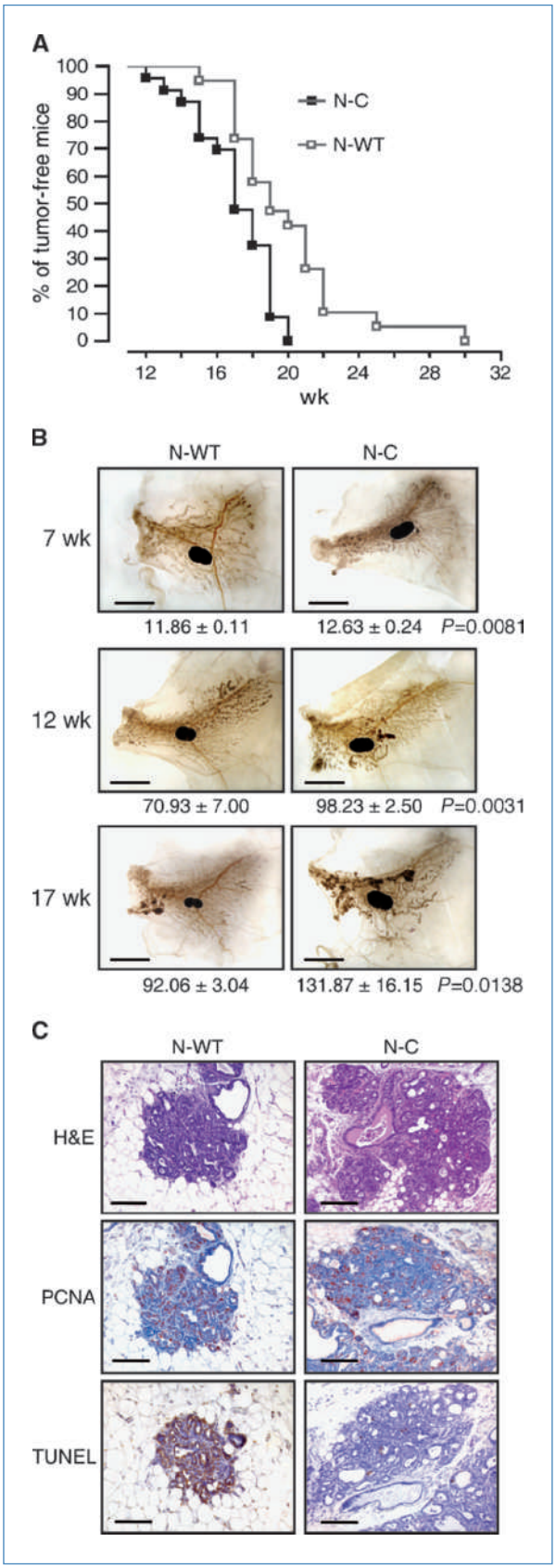

Histology and immunohistochemistry. Mammary tissue was processed as previously described (30). Formalin-fixed tissue sections were stained with H&E or overlaid with biotinylated goat anti-mouse and anti-rabbit immunoglobulin (Vector Laboratories) followed by avidin-biotin complex/alkaline phosphatase (DAKO). Terminal deoxynucleotidyl transferase-mediated dUTP nick-end labeling (TUNEL) was performed using ApopTag Plus Peroxidase *In situ* Apoptosis kit (Millipore).

Immunofluorescence. Cells plated on glass coverslips were washed in PBS, fixed in 4% paraformaldehyde, quenched with 50 mmol/L ammonium chloride, permeabilized with 0.3% Triton X-100 in PBS, saturated with 3% bovine serum albumin, and incubated with primary antibodies at room temperature for 1 h, followed by fluorescein- or rhodamine-labeled secondary antibodies (Sigma) or phalloidin (Sigma) and then by Hoechst-dye. An Axiovert 200M Zeiss microscope or the Axio-Observer-Z1 Zeiss microscope with the ApoTome system for optical sectioning were used. Images were acquired with MetaMorph software (Molecular Devices) or the AxioVision release 4.6.3 software (Carl Zeiss, Inc.), respectively.

Statistical analysis. Kaplan-Meier survival curves were analyzed by Prism4 (GraphPad software); *P* values were calculated using the log-rank test. All other *P* values were calculated using Student's *t* test (unpaired, two tailed).

Results

Stat3C knock-in mice display constitutive Stat3 nuclear localization, phosphorylation, and transcriptional activity. Mice carrying a mutant *Stat3C* allele have been generated by a knock-in strategy similar to the one previously described (ref. 25; Supplementary Fig. S1). Stat3 was expressed at physiologic levels in all tissues analyzed in both the homozygous and heterozygous mutant mice (Supplementary Fig. S2A). $Stat3^{C/C}$ mice died at young age due to immune defects,[7] whereas $Stat3^{C/WT}$ mice were viable and fertile.

[7] Unpublished observation.

Figure 1. Stat3C enhances Neu-mediated mammary gland tumorigenesis. A, Kaplan-Meier curve showing the percentage of N-WT (n = 20) or of N-C (n = 24) female mice free of palpable tumors as a function of age (P = 0.0014). B, ferric hematoxylin staining of WM mammary glands from N-C and N-WT mice at the indicated ages. Note the amplification of neoplastic lesions ranging from atypical hyperplasia to *in situ* and invasive carcinomas (dark dots and nodules) in the N-C mice. The central black oval areas are mammary lymph nodes (scale bar, 5 mm). Digital quantification of the neoplastic lesions (mean width in μm) in samples from three different animals per genotype is shown with the relative *P* values. C, histology (H&E) performed on mammary samples from 12-wk-old mice showing pseudoalveolar aggregates of the N-C tumor cells invading the surrounding fibroadipose tissue. Proliferation and apoptosis are evaluated by means of anti-PCNA (PCNA) and TUNEL staining (scale bar, 150 μm). B and C, representative images of sections from three independent animals per genotype.

Published OnlineFirst March 9, 2010; DOI: 10.1158/0008-5472.CAN-09-2840

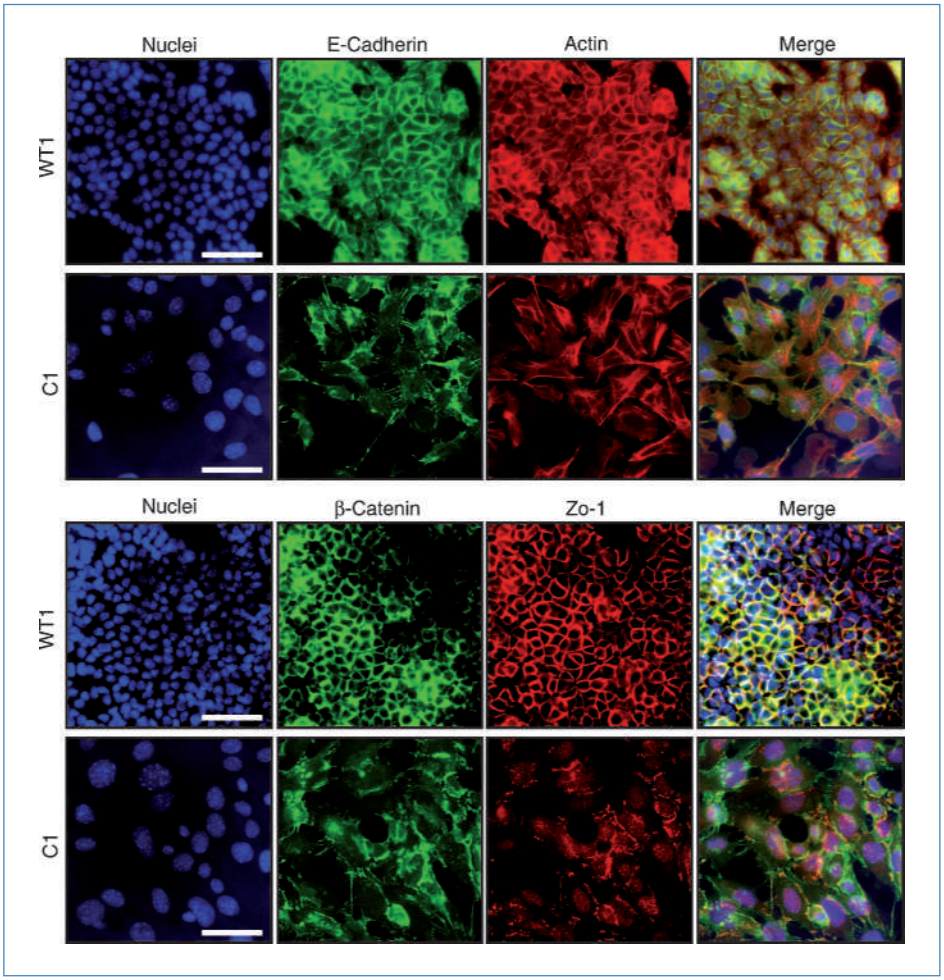

Figure 2. Disrupted distribution of cell-cell contacts in the C cell lines assessed by immunofluorescence staining. The C1 and WT1 tumor-derived cell lines were plated on coated glass slides and incubated with phalloidin-TRITC or with antibodies against E-cadherin, β-catenin (mouse monoclonal), or Zo-1 (rabbit polyclonal) followed by Hoechst staining and incubation with FITC-labeled anti-mouse or TRITC-labeled antirabbit antibodies. Note the less regular distribution of the epithelial markers and the absence of cortical actin/presence of actin stress fibers in the C1 cells. Scale bar, 20 μm.

Stat3C expressed by the knocked-in allele was indeed constitutively active. *Stat3*$^{C/C}$ mice displayed slightly enhanced Stat3 nuclear localization and tyrosine phosphorylation in the liver (Supplementary Fig. S2B), leading to significantly increased levels of several acute phase mRNAs, well-known Stat3 transcriptional targets (Supplementary Fig. S2D). Upon lipopolysaccharide (LPS)–mediated activation, nuclear localization of active, phosphorylated Stat3 was prolonged in the liver of the *Stat3*$^{C/C}$ mice (Supplementary Fig. S2C and not shown). Both basal and induced nuclear localization and phosphorylation were also increased in *Stat3*$^{C/C}$ primary mouse embryonic fibroblasts (MEF; Supplementary Fig. S2E), correlating with increased basal expression of a subset of known Stat3 target genes (Supplementary Fig. S2F). Both transcriptional activity and DNA binding affinity of the Stat3C protein were comparable with those of the wild-type form, as judged by normal, and sometimes prolonged, LPS- or IL-6–mediated induction of tested target genes in the liver or in MEF cells, respectively (not shown), and by EMSA competitions (Supplementary Fig. S2C).

Stat3C expression enhances Neu-mediated mammary gland tumorigenesis. Spontaneous tumor onset could not be assessed in aging *Stat3*$^{C/C}$ mice due to their early mortality. No preneoplastic lesions or spontaneously arising tumors were detected in heterozygous *Stat3*$^{C/WT}$ mice up to 24 months of age, and breast gland morphology was normal in virgin, pregnant, and lactating *Stat3*$^{C/WT}$ female mice.[7] We decided therefore to assess potential cooperation of one constitutively active *Stat3C* allele with the *Neu* oncogene in mammary tumorigenesis. NeuT mice, which develop multiple foci of atypical hyperplasia progressing to invasive metastasizing carcinoma by 22 to 27 weeks (30), were intercrossed with *Stat3*$^{C/WT}$ mice to obtain N-C and N-WT mice. N-C mice developed palpable tumors significantly earlier than their N-WT control littermates (Fig. 1A; $P = 0.0014$). This was also confirmed by the presence of more diffused and advanced neoplastic lesions in the N-C mice in WM mammary gland preparations performed at 7, 12, and 17 weeks of age (Fig. 1B). Analysis of sectioned WM preparations also revealed larger and more advanced tumor lesions (Fig. 1C), with normal proliferation rates as assessed by PCNA staining, but sensibly reduced TUNEL-positive apoptotic nuclei. In particular at 12 weeks, N-C mice already showed invasive carcinomas, with tumor cells grouped in solid masses and small

Published OnlineFirst March 9, 2010; DOI: 10.1158/0008-5472.CAN-09-2840

aggregates invading the surrounding fibroadipose tissue, whereas only atypical hyperplastic foci and few *in situ* carcinomas were detected in the N-WT mice (Fig. 1C; H&E).

Generation of tumor-derived cell lines. Neu protein levels and phosphorylation were similar in tumors of both genotypes (Supplementary Fig. S3C and D). Likewise, phosphorylation of both Stat3 and Stat5, another STAT factor often activated in breast tumors, could be detected in both N-C and N-WT tumors (Supplementary Fig. S3A, B), and no consistent differences were detected in the main biochemical pathways known to be involved in Neu-mediated mammary tumorigenesis, including the expression or activity of Pten, Akt, Gsk3-β, Src, and Erk (Supplementary Fig. S3E).

To generate a tool to identify the specific contribution of enhanced Stat3 activity to the malignancy of Neu-transformed breast tumor cells, three independent cell lines were derived from tumors of each genotype and named C or WT 1, 2, or 3. All cell lines maintained Neu expression and activity through at least 10 passages in culture (Supplementary Fig. S3H and I). All three C cell lines displayed increased nuclear, phosphorylated Stat3, suggesting enhanced activity of the *Stat3C* allele, whereas levels of phosphorylated Stat5 seemed unchanged (Supplementary Fig. S3F, G and S5A). Accordingly, the mRNA levels for SOCS3, a typical Stat3 target, were increased (Supplementary Fig. S4). C and WT cell lines did not display any significant difference in Pten, Akt, Gsk3-β, Src, and Erk expression or activation (Supplementary Fig. S3J), except that both WT-1 and -2 cells underwent loss of Pten expression, a feature never displayed by the C cell lines even after >30 passages (Supplementary Fig. S5B). Pten loss occurred reproducibly between the first and second passage in culture in the WT-2 cell line, which as a consequence acquired faster growth rates (not shown). Cells were therefore routinely checked for Pten expression before all experiments described.

C and WT cell lines did not differ significantly in terms of proliferation or resistance to starvation-mediated apoptosis (data not shown). This is not surprising though in apparent contradiction with the observed reduced apoptotic index of the N-C tumors, because *in vitro* stabilization of tumor cells involves the selection of cells able to survive and can thus mask differences evident *in vivo*. However, all WT cell lines exhibited a more differentiated phenotype, growing in tight islets with well-organized and continuous adherent and tight

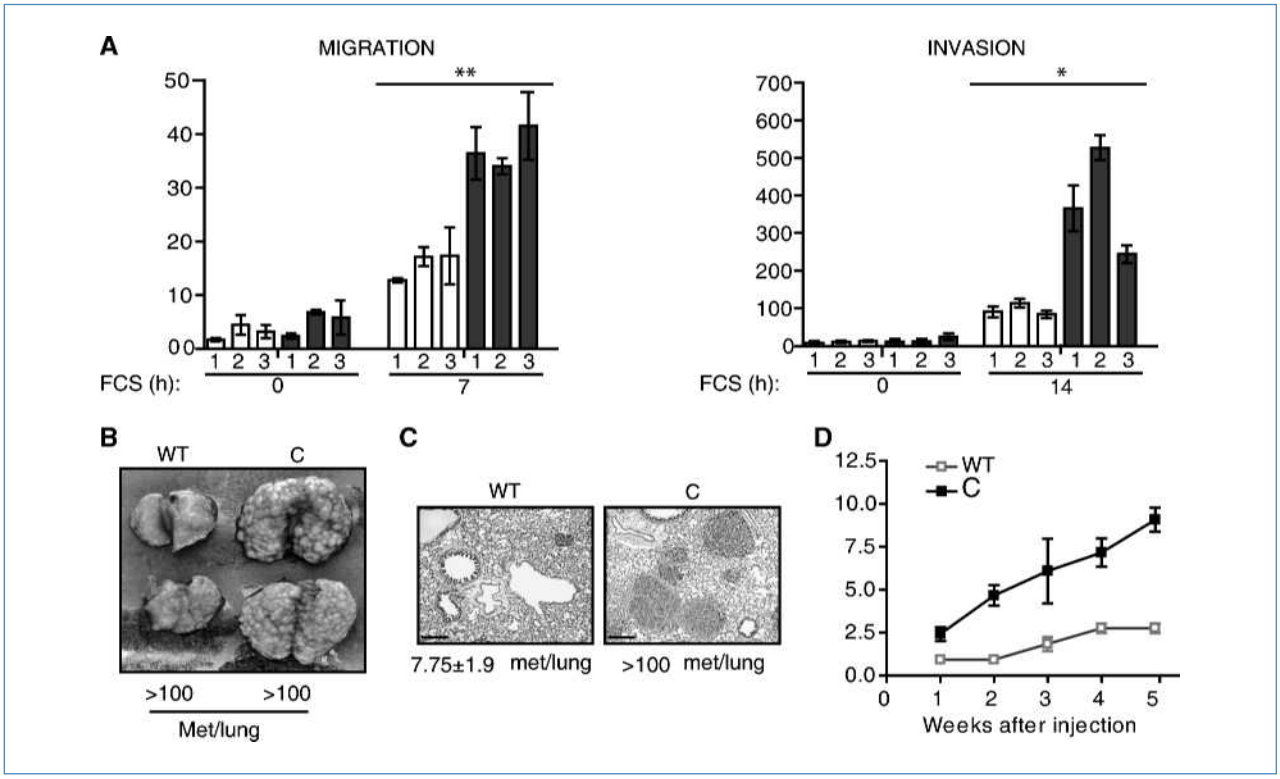

Figure 3. The C cell lines display increased invasivity both *in vitro* and *in vivo*. A, the indicated tumor-derived cell lines were subjected to Transwell migration assay (left) or to Matrigel invasion assay (right) in response to FCS. The histograms (C, filled bars; WT, empty bars) show the mean number ± SEM of migrated cells per microscopic field (20×, $P = 0.0013$) or the mean number ± SEM of invading cells per transwell insert expressed as a percentage of the value obtained with WT1 stimulated cells ($P = 0.003$). One representative of three independently performed experiments is shown in each case. B-D, *in vivo* tumorigenesis. 1×10^5 WT1 or C1 cells were injected either in the tail vein (B, C) or s.c. in the right flank (D) of nude mice. Lungs ($n = 4$) were dissected 5 (B) or 3 (C) wk after injection and either macroscopically photographed (B) or fixed, sectioned, and stained with H&E (C; scale bar, 1 mm). The mean number of metastases per lung is shown. D, tumor size was measured weekly with a caliper, and data are shown as mean size ± SEM of tumors in six mice per cell line ($P = 0.0097$).

Published OnlineFirst March 9, 2010; DOI: 10.1158/0008-5472.CAN-09-2840

junctions, as shown by staining of E-cadherin, β-catenin, and Zo-1 (Fig. 2; Supplementary Fig. S6). Accordingly, actin fibers were mainly located in the cortical region. Despite similar expression levels of the same epithelial markers detected by Western blot (not shown), all C cell lines displayed discontinuous E-cadherin, β-catenin, and Zo-1 distribution, suggesting less organized cell-cell contacts. In keeping with their less differentiated, spindle-like phenotype, all C cells showed reduced cortical actin and evident actin stress-fibers that were never detected in the WT cells.

Stat3C enhances migration, invasivity, and metastatic potential of NeuT tumor cells. Migration and extracellular matrix invasion of the C and WT cell lines were assessed by Transwell assays with or without a Matrigel coating (Fig. 3A). Migration was at least doubled in all C cell lines ($P = 0.0013$), which also showed strongly enhanced Matrigel invasion potential ($P = 0.03$), suggesting higher invasive and metastatic activity. To evaluate these parameters *in vivo*, C1 or WT1 cells were injected i.v. into nude mice and the formation of lung metastases was assessed after 3 or 5 weeks of injection. C1 cells displayed a strongly enhanced metastatic potential, producing more and faster growing lung metastases both at 5 (Fig. 3B) and 3 weeks (Fig. 3C). Similar results were obtained with the other cell lines (data not shown). Of note, WT2 cells were excluded from this analysis to avoid nonspecific interference of their Pten loss. C1 cells were also able to produce s.c. tumors displaying fast and regular growth and reaching a diameter of 10 mm 5 weeks after injection, whereas tumors produced by the WT1 cells grew much slower and never reached the 10-mm size (Fig. 3D and not shown).

Gene expression profiling of the C and WT cell lines. Gene expression profiles of all cell lines were compared using an Illumina microarray platform. The microarray raw data have been deposited in National Center for Biotechnology Information Gene Expression Omnibus (accession no. GSE17182). The rank products function (31) was used to produce a list of 23 upregulated genes, most of which are functionally related to growth control and/or tumor biology (Supplementary Table S1). Consistent differential expression was confirmed in 4 of 10 tested genes, namely Cten/tensin 4, galectin 3 (Lgals3), ly6/Plaur domain containing 3 (Lypd3), and proliferin 2 (Fig. 4A and not shown). Further analysis of the microarray experiment, excluding the WT2 cells on the ground of their Pten loss (not shown), suggested differential expression also of Twist 1, a known Stat3 target gene involved in EMT induction (17, 32), confirmed by reverse transcription–PCR (RT-PCR) analysis (Fig. 4A). In addition, both Cten and Twist 1 also displayed significantly higher expression in the N-C tumors compared with their N-WT controls (Fig. 4B).

Cten partly mediates the aggressive phenotype of the C cells and is a Stat3 target also in MCF10 cells. Because Cten, the most consistently upregulated gene in both cell lines and tumors, is implicated in EGF-dependent mammary cell migration (33), we decided to assess its contribution to the observed phenotype of the C cell lines. siRNA treatment could efficiently reduce Cten levels to ~20% in both the C1

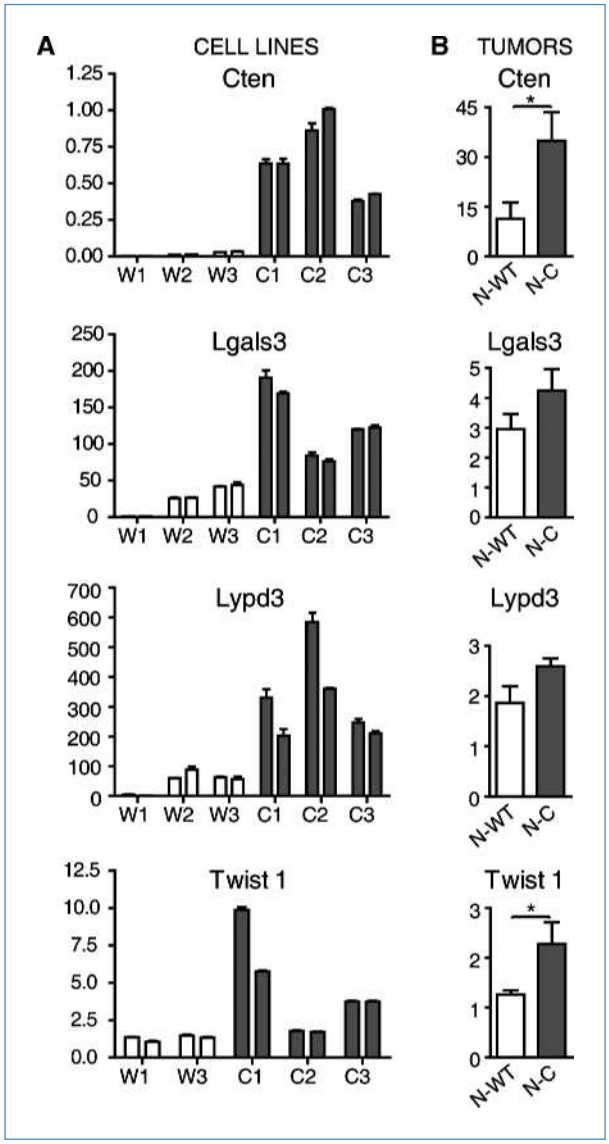

Figure 4. Genes differentially expressed in the cell lines and tumors. Total RNA was extracted from cell lines (A) or tumors (B) of the indicated genotype and subjected to reverse transcription followed by TaqMan real-time PCR analysis. Results are shown as mean values ± SEM of experimental triplicates and are representative of six independent experiments (A) and as mean values ± SEM of nine individual tumors per genotype (B). *, statistically significant differences: Cten, $P = 0.032$; Twist 1, $P = 0.0351$.

and C2 cell lines (Fig. 5A and B; Supplementary Fig. S7A), resulting in significant inhibition of cell migration (Fig. 5C; Supplementary Fig. S7B) and, intriguingly, in partial reversion of both Zo-1 and β-catenin cell surface distribution (Fig. 5D). Cells adopted a more epithelial phenotype and displayed enhanced and more continuous cortical localization of both epithelial markers, correlating with tighter cell-cell contacts as already evident in the phase-contrast images.

Both Cten overexpression and increased cell migration were indeed dependent on Stat3 activity, because treatment

Published OnlineFirst March 9, 2010; DOI: 10.1158/0008-5472.CAN-09-2840

of C1 cells with the specific Stat3 inhibitor S3I (26) coordinately and strongly reduced Stat3 (but not Stat5) phosphorylation, Cten levels, and cell migration (Fig. 6A and B). Importantly, Stat5 phosphorylation was unaffected by S3I treatment (Fig. 6A). In addition, we observed that IL-6 treatment could efficiently upregulate CTEN in nontransformed MCF10 human mammary cells, correlating with prolonged phosphorylation of STAT3, but not of STAT5 (Fig. 6C; Supplementary Fig. S8). Of note, IL-6–mediated CTEN induction was only slightly slower than that triggered by EGF (Supplementary Fig. S8) and was clearly dependent on STAT3 activity, because it was completely abrogated by the S3I inhibitor (Fig. 6D), indicating that the ability to trigger CTEN induction is a feature of both constitutively active and inflammation-activated Stat3.

Discussion

The constitutive activation of STAT3 observed in many tumors of distinct origin, including the breast, suggests that STAT3 transcriptional activity may provide essential functions to tumor cells (3). Their identification is complicated by the variable degrees of STAT3 activity and addiction detected in individual tumors, likely reflecting the different combinations of tumorigenic pathways able to trigger STAT3 phosphorylation active in individual cases. Our model provides an experimental system wherein the contribution of enhanced Stat3 activity to oncogene-driven tumorigenesis can be directly tested by comparing phenotype and gene expression profiles of tumors carrying normal or activated Stat3.

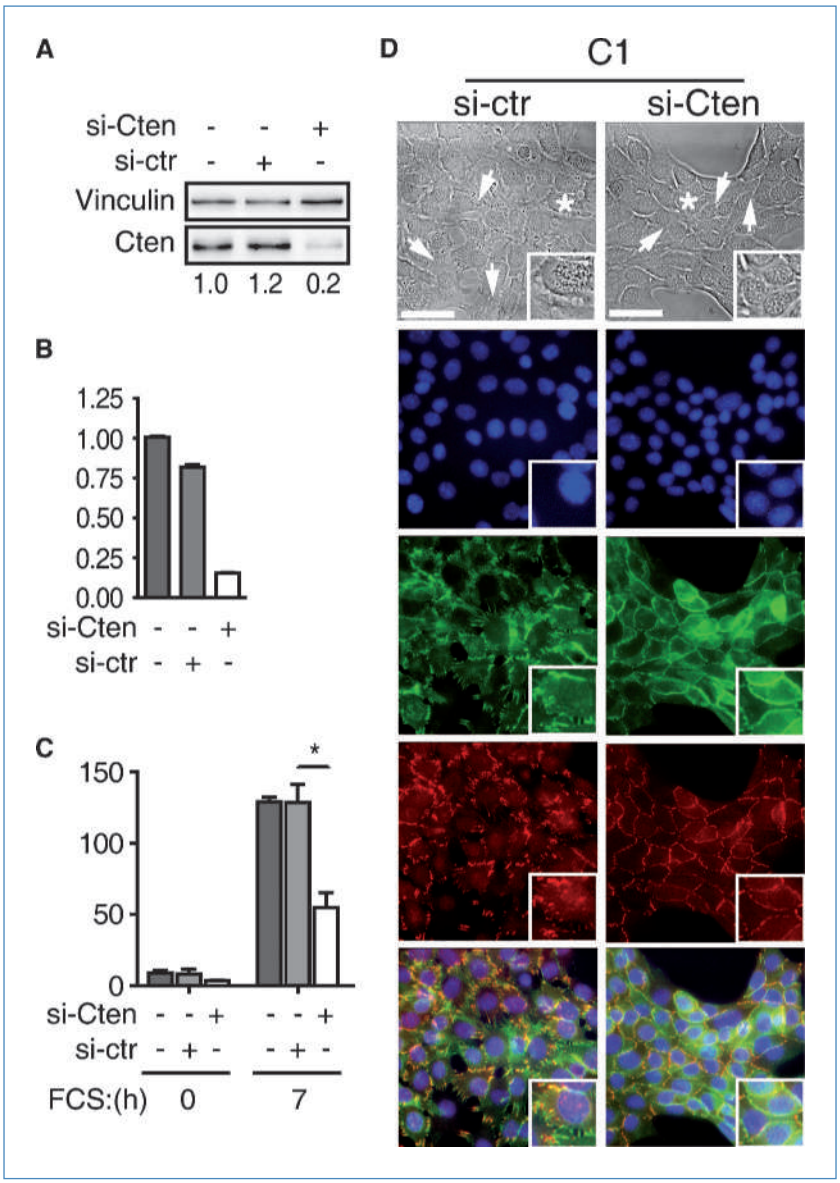

Figure 5. Cten silencing partially reverts the aggressive phenotype of C cells. A and B, C1 cells were treated for 72 h with the SMARTpool siRNA reagent (Accell System, Dharmacon) against Cten (si-Cten) or with a control Accell nontargeting siRNA (si-ctr). A, protein levels were assessed by Western blot of whole protein lysates with the indicated antibodies. Numbers indicate the relative quantification of Cten expression upon normalization to Vinculin. B, Cten mRNA quantification by TaqMan RT-PCR analysis (mean ± SEM of two samples, performed in triplicate, from one of two independent experiments). C and D, silenced cells were subjected to a Transwell migration assay in response to FCS (C) or to immunofluorescence staining (D). C, values are shown as mean numbers ± SEM of migrated cells per microscopic field (20×) of triplicates in one representative of two independently performed experiments ($P < 0,05$). D, phase contrast and immunofluorescence images of silenced C1 cells from A and B. Arrows in the phase contrast images indicate particularly evident discontinuous (si-ctr) versus tight (si-Cten) cell-cell contacts. Nuclei are shown in blue, β-catenin in green, and Zo-1 in red. The areas indicated by an asterisk in the phase contrast images are magnified in the insets (4× magnification). Scale bar, 20 μm.

Published OnlineFirst March 9, 2010; DOI: 10.1158/0008-5472.CAN-09-2840

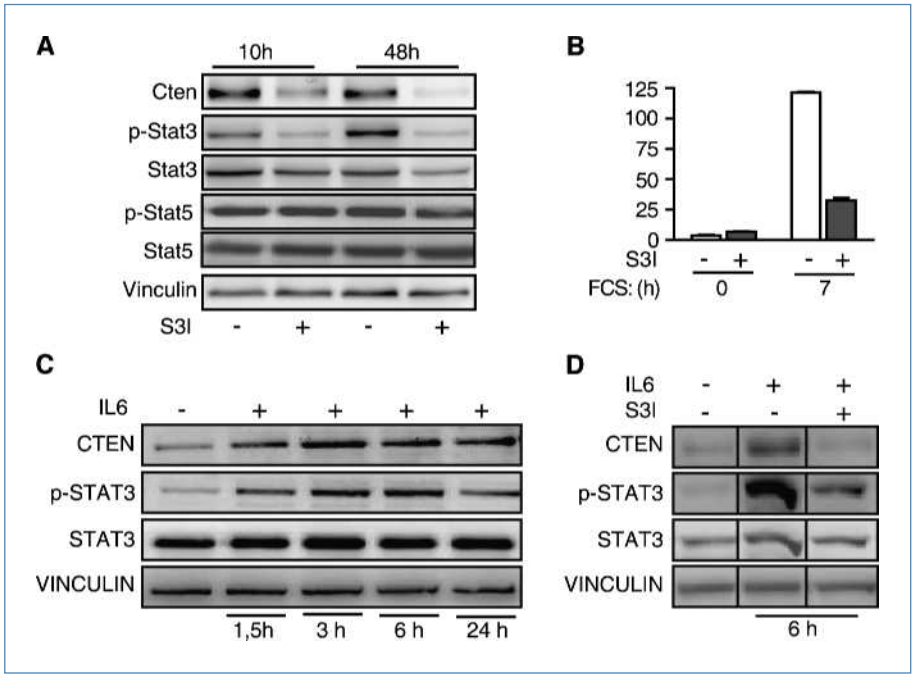

Figure 6. Cten expression is dependent on Stat3 activity. A and B, C1 cells were treated or not with the Stat3-specific inhibitor S3I for 10 or 48 h and analyzed by Western blot with the indicated antibodies (A) or treated for 48 h and successively subjected to a Transwell migration assay in response to FCS (B). C and D, Western blot analysis of whole protein extracts from MCF10 cells treated with IL-6 for the indicated times (C) or treated with IL-6 ± the Stat3 inhibitor S3I for 6 h (D).

We show here for the first time that Stat3C does behave as a constitutively active form even when not overexpressed. Under these conditions, which simulate the continuous activity of Stat3 observed in many tumors, Stat3C fails to induce tumorigenesis on its own but can cooperate with the *Neu* oncogene in mammary tumorigenesis. Stat3 is only slightly activated downstream of Neu, but its activity is enhanced in the N-C mice, mainly acting at two levels: (*a*) protection from apoptosis, which is likely to contribute to the earlier tumor onset observed, and (*b*) promotion of tumor aggressiveness and metastatic potential. Unfortunately, the MMTV-*Neu* transgenic model is not well suited for the analysis of spontaneous lung metastases in our system. These occurred very late and with variable penetrance, often after the N-C mice had to be sacrificed for humane reasons.[8] However, the generation of cell lines allowed us to explore the contribution of Stat3C to invasion/motility of Neu-transformed tumor cells both at the phenotypic and molecular level. All C cell lines displayed significantly enhanced migration and invasion *in vitro* and increased tumorigenic potential *in vivo*, correlating with profoundly modified cytoskeletal and cell-cell contacts organization affecting both adherent and tight junctions, identified by immunostaining of their essential components E-cadherin, β-catenin, or Zo-1 (34). This correlated with dramatically reduced cortical actin and with the appearance of abundant actin stress fibers that are important to exert the pulling forces resulting in cell movement (35). Remarkably, four of five genes confirmed to be expressed at higher levels in all three C cell lines (i.e., Cten, Lgals3, Lypd3, and Twist 1) are known to play a role in regulating cell migration and/or tumor metastasis, and all four tend to be expressed at higher levels also in the N-C tumors. Twist 1 is a well-known Stat3 transcriptional target involved in the induction of tumor invasivity and EMT (17, 32), whereas Cten, Lgals3, or Lypd3 have never been associated with Stat3.

Cten, the most consistently upregulated gene in both cell lines and tumors, is an atypical tensin family member lacking the actin-binding domain (29) and was recently shown to be upregulated by EGF in mammary cells and to mediate EGF-induced migration (33). Moreover, Cten was reported to promote colon cancer tumorigenicity and cell motility (36, 37), and its overexpression correlated with increasing tumor stage in thymomas, lung tumors, and gastric tumors (38–40), all of which have been reported to display constitutive Stat3 activity. We showed that Cten upregulation mediates both increased migration and disrupted distribution of cell junction markers of C cells and is clearly dependent on Stat3, as it was abolished by Stat3 inhibition. Inflammatory signals in the tumor microenvironment are well-recognized pathogenic factors in many types of malignancies, and recently both autocrine and paracrine production of the proinflammatory cytokine IL-6 were shown to promote Stat3-dependent tumorigenesis (7, 41). Taken together with the identification of Cten as a Stat3-dependent mediator of migration, our observation that IL-6 can induce CTEN in a STAT3-dependent way in MCF10 cells suggests that indeed CTEN may represent an important functional mediator in the loop inflammation-Stat3-migration/metastasis. Moreover, CTEN expression in human breast tumors was shown to correlate with high EGFR and HER2 levels, loss of estrogen receptor, high tumor grade, and lymph node metastasis and was particularly elevated in the extremely aggressive and invasive inflammatory

[8] I. Barbieri and T. Pannellini, unpublished observations.

Published OnlineFirst March 9, 2010; DOI: 10.1158/0008-5472.CAN-09-2840

breast cancers (33). In this context, CTEN may provide a crucial point of functional convergence between inflammation-induced constitutively enhanced Stat3 activity, altered EGFR, and/or HER2-mediated signaling and invasion of the surrounding tissues and lymph nodes. Our data support the idea of Stat3 playing an essential role in metastasis formation downstream of Neu (21, 22, 42) and provide further insights into the molecular mechanisms linking Stat3 activation, inflammatory response, and migration/metastasis.

Disclosure of Potential Conflicts of Interest

No potential conflicts of interest were disclosed.

Acknowledgments

We thank E. Hirsch, G. Forni, P.P. Pandolfi, and S. Cabodi for critically reading the manuscript, S.H. Lo for the kind gift of the anti-CTEN antibody, and L. Silengo for continuous support.

Grant Support

Italian Cancer Research Association (AIRC), Italian Ministry for University and Research PRIN and FIRB, Ricerca Finalizzata Piemonte, Progetto Alfieri from CRT Foundation, and Association for International Cancer Research.

The costs of publication of this article were defrayed in part by the payment of page charges. This article must therefore be hereby marked *advertisement* in accordance with 18 U.S.C. Section 1734 solely to indicate this fact.

Received 07/31/2009; revised 11/30/2009; accepted 01/11/2010; published OnlineFirst 03/09/2010.

References

1. Fernandes A, Hamburger AW, Gerwin BI. ErbB-2 kinase is required for constitutive stat 3 activation in malignant human lung epithelial cells. Int J Cancer 1999;83:564–70.
2. Turkson J, Jove R. STAT proteins: novel molecular targets for cancer drug discovery. Oncogene 2000;19:6613–26.
3. Kortylewski M, Jove R, Yu H. Targeting STAT3 affects melanoma on multiple fronts. Cancer Metastasis Rev 2005;24:315–27.
4. Al Zaid Siddiquee K, Turkson J. STAT3 as a target for inducing apoptosis in solid and hematological tumors. Cell Res 2008;18: 254–67.
5. Pensa S, Regis G, Boselli D, Novelli F, Poli V. STAT1 and STAT3 in tumorigenesis: two sides of the same coin? In: Stephanou A, editor. JAK-STAT Pathway in Disease. Austin: Landes Bioscience; 2009, p. 100–21.
6. Yu H, Kortylewski M, Pardoll D. Crosstalk between cancer and immune cells: role of STAT3 in the tumour microenvironment. Nat Rev Immunol 2007;7:41–51.
7. Bromberg J, Wang TC. Inflammation and cancer: IL-6 and STAT3 complete the link. Cancer Cell 2009;15:79–80.
8. Bromberg JF, Wrzeszczynska MH, Devgan G, et al. Stat3 as an oncogene. Cell 1999;98:295–303.
9. Dechow TN, Pedranzini L, Leitch A, et al. Requirement of matrix metalloproteinase-9 for the transformation of human mammary epithelial cells by Stat3-C. Proc Natl Acad Sci U S A 2004;101: 10602–7.
10. Azare J, Leslie K, Al-Ahmadie H, et al. Constitutively activated Stat3 induces tumorigenesis and enhances cell motility of prostate epithelial cells through integrin β6. Mol Cell Biol 2007;27:4444–53.
11. Chan KS, Sano S, Kataoka K, et al. Forced expression of a constitutively active form of Stat3 in mouse epidermis enhances malignant progression of skin tumors induced by two-stage carcinogenesis. Oncogene 2008;27:1087–94.
12. Li Y, Du H, Qin Y, Roberts J, Cummings OW, Yan C. Activation of the signal transducers and activators of the transcription 3 pathway in alveolar epithelial cells induces inflammation and adenocarcinomas in mouse lung. Cancer Res 2007;67:8494–503.
13. Diaz N, Minton S, Cox C, et al. Activation of stat3 in primary tumors from high-risk breast cancer patients is associated with elevated levels of activated SRC and survivin expression. Clin Cancer Res 2006; 12:20–8.
14. Gritsko T, Williams A, Turkson J, et al. Persistent activation of stat3 signaling induces survivin gene expression and confers resistance to apoptosis in human breast cancer cells. Clin Cancer Res 2006;12: 11–9.
15. Leslie K, Lang C, Devgan G, et al. Cyclin D1 is transcriptionally regulated by and required for transformation by activated signal transducer and activator of transcription 3. Cancer Res 2006;66:2544–52.
16. Berclaz G, Altermatt HJ, Rohrbach V, Siragusa A, Dreher E, Smith PD. EGFR dependent expression of STAT3 (but not STAT1) in breast cancer. Int J Oncol 2001;19:1155–60.
17. Lo HW, Hsu SC, Xia W, et al. Epidermal growth factor receptor cooperates with signal transducer and activator of transcription 3 to induce epithelial-mesenchymal transition in cancer cells via up-regulation of TWIST gene expression. Cancer Res 2007;67:9066–76.
18. Menard S, Balsari A, Tagliabue E, et al. Biology, prognosis and response to therapy of breast carcinomas according to HER2 score. Ann Oncol 2008;19:1706–12.
19. Muller WJ, Sinn E, Pattengale PK, Wallace R, Leder P. Single-step induction of mammary adenocarcinoma in transgenic mice bearing the activated c-neu oncogene. Cell 1988;54:105–15.
20. Marcotte R, Muller WJ. Signal transduction in transgenic mouse models of human breast cancer-implications for human breast cancer. J Mammary Gland Biol Neoplasia 2008;13:323–35.
21. Barbieri I, Quaglino E, Maritano D, et al. Stat3 is required for anchorage-independent growth and metastasis but not for mammary tumor development downstream of the ErbB-2 oncogene. Mol Carcinog 2010;49:114–20.
22. Ranger JJ, Levy DE, Shahalizadeh S, Hallett M, Muller WJ. Identification of a Stat3-dependent transcription regulatory network involved in metastatic progression. Cancer Res 2009;69:6823–30.
23. Nanni P, Pupa SM, Nicoletti G, et al. p185(neu) protein is required for tumor and anchorage-independent growth, not for cell proliferation of transgenic mammary carcinoma. Int J Cancer 2000;87: 186–94.
24. Schiavone D, Dewilde S, Vallania F, Turkson J, Di Cunto F, Poli V. The RhoU/Wrch1 Rho GTPase gene is a common transcriptional target of both the gp130/STAT3 and Wnt-1 pathways. Biochem J 2009; 421:283–92.
25. Maritano D, Sugrue ML, Tininini S, et al. The STAT3 isoforms α and β have unique and specific functions. Nat Immunol 2004;5:401–9.
26. Siddiquee K, Zhang S, Guida WC, et al. Selective chemical probe inhibitor of Stat3, identified through structure-based virtual screening, induces antitumor activity. Proc Natl Acad Sci U S A 2007; 104:7391–6.
27. Alonzi T, Maritano D, Gorgoni B, Rizzuto G, Libert C, Poli V. Essential role of STAT3 in the control of the acute-phase response as revealed by inducible gene inactivation in the liver. Mol Cell Biol 2001;21: 1621–32.
28. Vallania F, Schiavone D, Dewilde S, et al. Genome-wide discovery of functional transcription factor binding sites by comparative genomics: the case of Stat3. Proc Natl Acad Sci U S A 2009; 106:5117–22.
29. Lo SH, Lo TB. Cten, a COOH-terminal tensin-like protein with prostate restricted expression, is down-regulated in prostate cancer. Cancer Res 2002;62:4217–21.
30. Di Carlo E, Diodoro MG, Boggio K, et al. Analysis of mammary carcinoma onset and progression in HER-2/neu oncogene transgenic mice reveals a lobular origin. Lab Invest 1999;79:1261–9.
31. Breitling R, Armengaud P, Amtmann A, Herzyk P. Rank products: a simple, yet powerful, new method to detect differentially regulated

Published OnlineFirst March 9, 2010; DOI: 10.1158/0008-5472.CAN-09-2840

genes in replicated microarray experiments. FEBS Lett 2004;573:83–92.
32. Cheng GZ, Zhang WZ, Sun M, et al. Twist is transcriptionally induced by activation of STAT3 and mediates STAT3 oncogenic function. J Biol Chem 2008;283:14665–73.
33. Katz M, Amit I, Citri A, et al. A reciprocal tensin-3-cten switch mediates EGF-driven mammary cell migration. Nat Cell Biol 2007;9:961–9.
34. Niessen CM. Tight junctions/adherens junctions: basic structure and function. J Investig Dermatol 2007;127:2525–32.
35. Pellegrin S, Mellor H. Actin stress fibres. J Cell Sci 2007;120:3491–9.
36. Albasri A, Seth R, Jackson D, et al. C-terminal Tensin-like (CTEN) is an oncogene which alters cell motility possibly through repression of E-cadherin in colorectal cancer. J Pathol 2009;218:57–65.
37. Liao YC, Chen NT, Shih YP, Dong Y, Lo SH. Up-regulation of C-terminal tensin-like molecule promotes the tumorigenicity of colon cancer through β-catenin. Cancer Res 2009;69:4563–6.
38. Sasaki H, Yukiue H, Kobayashi Y, Fukai I, Fujii Y. Cten mRNA expression is correlated with tumor progression in thymoma. Tumour Biol 2003;24:271–4.
39. Sakashita K, Mimori K, Tanaka F, et al. Prognostic relevance of Tensin4 expression in human gastric cancer. Ann Surg Oncol 2008;15:2606–13.
40. Sasaki H, Moriyama S, Mizuno K, et al. Cten mRNA expression was correlated with tumor progression in lung cancers. Lung Cancer (Amsterdam, the Netherlands) 2003;40:151–5.
41. Grivennikov S, Karin M. Autocrine IL-6 signaling: a key event in tumorigenesis? Cancer Cell 2008;13:7–9.
42. Guo W, Pylayeva Y, Pepe A, et al. β4 integrin amplifies ErbB2 signaling to promote mammary tumorigenesis. Cell 2006;126:489–502.

Cancer Research

Correction: Online Publication Dates for *Cancer Research* April 15, 2010 Articles

The following articles in the April 15, 2010 issue of *Cancer Research* were published with an online publication date of April 6, 2010 listed, but were actually published online on April 13, 2010:

Garmy-Susini B, Avraamides CJ, Schmid MC, Foubert P, Ellies LG, Barnes L, Feral C, Papayannopoulou T, Lowy A, Blair SL, Cheresh D, Ginsberg M, Varner JA. Integrin $\alpha4\beta1$ signaling is required for lymphangiogenesis and tumor metastasis. Cancer Res 2010;70:3042–51. Published OnlineFirst April 13, 2010. doi:10.1158/0008-5472.CAN-09-3761.

Vincent J, Mignot G, Chalmin F, Ladoire S, Bruchard M, Chevriaux A, Martin F, Apetoh L, Rébé C, Ghiringhelli F. 5-Fluorouracil selectively kills tumor-associated myeloid-derived suppressor cells resulting in enhanced T cell-dependent antitumor immunity. Cancer Res 2010;70:3052–61. Published OnlineFirst April 13, 2010. doi:10.1158/0008-5472.CAN-09-3690.

Nagasaka T, Rhees J, Kloor M, Gebert J, Naomoto Y, Boland CR, Goel A. Somatic hypermethylation of *MSH2* is a frequent event in Lynch syndrome colorectal cancers. Cancer Res 2010;70:3098–108. Published OnlineFirst April 13, 2010. doi:10.1158/0008-5472.CAN-09-3290.

He X, Ota T, Liu P, Su C, Chien J, Shridhar V. Downregulation of HtrA1 promotes resistance to anoikis and peritoneal dissemination of ovarian cancer cells. Cancer Res 2010;70:3109–18. Published OnlineFirst April 13, 2010. doi:10.1158/0008-5472.CAN-09-3557.

Fiorentino M, Judson G, Penney K, Flavin R, Stark J, Fiore C, Fall K, Martin N, Ma J, Sinnott J, Giovannucci E, Stampfer M, Sesso HD, Kantoff PW, Finn S, Loda M, Mucci L. Immunohistochemical expression of BRCA1 and lethal prostate cancer. Cancer Res 2010;70:3136–9. Published OnlineFirst April 13, 2010. doi:10.1158/0008-5472.CAN-09-4100.

Veronese A, Lupini L, Consiglio J, Visone R, Ferracin M, Fornari F, Zanesi N, Alder H, D'Elia G, Gramantieri L, Bolondi L, Lanza G, Querzoli P, Angioni A, Croce CM, Negrini M. Oncogenic role of *miR-483-3p* at the *IGF2/483* locus. Cancer Res 2010;70:3140–9. Published OnlineFirst April 13, 2010. doi:10.1158/0008-5472.CAN-09-4456.

Lu W, Zhang G, Zhang R, Flores LG II, Huang Q, Gelovani JG, Li C. Tumor site–specific silencing of *NF-κB p65* by targeted hollow gold nanosphere–mediated photothermal transfection. Cancer Res 2010;70:3177–88. Published OnlineFirst April 13, 2010. doi:10.1158/0008-5472.CAN-09-3379.

Geng H, Rademacher BL, Pittsenbarger J, Huang C-Y, Harvey CT, Lafortune MC, Myrthue A, Garzotto M, Nelson PS, Beer TM, Qian DZ. ID1 enhances docetaxel cytotoxicity in prostate cancer cells through inhibition of p21. Cancer Res 2010;70:3239–48. Published OnlineFirst April 13, 2010. doi:10.1158/0008-5472.CAN-09-3186.

Yoo BK, Chen D, Su Z-z, Gredler R, Yoo J, Shah K, Fisher PB, Sarkar D. Molecular mechanism of chemoresistance by astrocyte elevated gene-1. Cancer Res 2010;70:3249–58. Published OnlineFirst April 13, 2010. doi:10.1158/0008-5472.CAN-09-4009.

Lu ZH, Shvartsman MB, Lee AY, Shao JM, Murray MM, Kladney RD, Fan D, Krajewski S, Chiang GG, Mills GB, Arbeit JM. Mammalian target of rapamycin activator RHEB is frequently overexpressed in human carcinomas and is critical and sufficient for skin epithelial carcinogenesis. Cancer Res 2010;70:3287–98. Published OnlineFirst April 13, 2010. doi:10.1158/0008-5472.CAN-09-3467.

Hattermann K, Held-Feindt J, Lucius R, Müerköster SS, Penfold MET, Schall TJ, Mentlein R. The chemokine receptor CXCR7 is highly expressed in human glioma cells and mediates antiapoptotic effects. Cancer Res 2010;70:3299–308. Published OnlineFirst April 13, 2010. doi:10.1158/0008-5472.CAN-09-3642.

Nadiminty N, Lou W, Sun M, Chen J, Yue J, Kung H-J, Evans CP, Zhou Q, Gao AC. Aberrant activation of the androgen receptor by NF-κB2/p52 in prostate cancer cells. Cancer Res 2010;70:3309–19. Published OnlineFirst April 13, 2010. doi:10.1158/0008-5472.CAN-09-3703.

Acu ID, Liu T, Suino-Powell K, Mooney SM, D'Assoro AB, Rowland N, Muotri AR, Correa RG, Niu Y, Kumar R, Salisbury JL. Coordination of centrosome homeostasis and DNA repair is intact in MCF-7 and disrupted in MDA-MB 231 breast cancer cells. Cancer Res 2010;70:3320–8. Published OnlineFirst April 13, 2010. doi:10.1158/0008-5472.CAN-09-3800.

McFarlane C, Kelvin AA, de la Vega M, Govender U, Scott CJ, Burrows JF, Johnston JA. The deubiquitinating enzyme USP17 is highly expressed in tumor biopsies, is cell cycle regulated, and is required for G_1-S progression. Cancer Res 2010;70:3329–39. Published OnlineFirst April 13, 2010. doi:10.1158/0008-5472.CAN-09-4152.

Dudka AA, Sweet SMM, Heath JK. Signal transducers and activators of transcription-3 binding to the fibroblast growth factor receptor is activated by receptor amplification. Cancer Res 2010;70:3391–401. Published OnlineFirst April 13, 2010. doi:10.1158/0008-5472.CAN-09-3033.

Cho SY, Xu M, Roboz J, Lu M, Mascarenhas J, Hoffman R. The effect of CXCL12 processing on $CD34^+$ cell migration in myeloproliferative neoplasms. Cancer Res 2010;70:3402–10. Published OnlineFirst April 13, 2010. doi:10.1158/0008-5472.CAN-09-3977.

Published OnlineFirst 05/11/2010.

doi: 10.1158/0008-5472.CAN-10-1347

AACR American Association for Cancer Research

Cancer Research

The Journal of Cancer Research (1916–1930) | The American Journal of Cancer (1931–1940)

Constitutively Active Stat3 Enhances Neu-Mediated Migration and Metastasis in Mammary Tumors via Upregulation of Cten

Isaia Barbieri, Sara Pensa, Tania Pannellini, et al.

Cancer Res 2010;70:2558-2567. Published OnlineFirst March 9, 2010.